Smoluchowski ripening of Ag islands on Ag(100)

C. R. Stoldt, C. J. Jenks, P. A. Thiel, A. M. Cadilhe, and J. W. Evans

Citation: The Journal of Chemical Physics **111**, 5157 (1999); doi: 10.1063/1.479770
View online: http://dx.doi.org/10.1063/1.479770
View Table of Contents: http://scitation.aip.org/content/aip/journal/jcp/111/11?ver=pdfcov
Published by the AIP Publishing

Smoluchowski ripening of Ag islands on Ag(100)

C. R. Stoldt, C. J. Jenks, and P. A. Thiel
Department of Chemistry and Ames Laboratory, Iowa State University, Ames, Iowa 50011

A. M. Cadilhe
IPRT and Ames Laboratory, Iowa State University, Ames, Iowa 50011

J. W. Evans[a)]
Department of Mathematics and Ames Laboratory, Iowa State University, Ames, Iowa 50011

(Received 1 March 1999; accepted 22 June 1999)

Using scanning tunneling microscopy, we study the post-deposition coarsening of distributions of large, two-dimensional Ag islands on a perfect Ag(100) surface at 295 K. The coarsening process is dominated by diffusion, and subsequent collision and coalescence of these islands. To obtain a comprehensive characterization of the coarsening kinetics, we perform *tailored families* of experiments, systematically varying the initial value of the average island size by adjusting the amount of Ag deposited (up to 0.25 ML). Results unambiguously indicate a strong decrease in island diffusivity with increasing island size. An estimate of the size scaling exponent follows from a mean-field Smoluchowski rate equation analysis of experimental data. These rate equations also predict a *rapid* depletion in the initial population of smaller islands. This leads to narrowing of the size distribution scaling function from its initial form, which is determined by the process of island nucleation and growth during deposition. However, for later times, a steady increase in the width of this scaling function is predicted, consistent with observed behavior. Finally, we examine the evolution of Ag adlayers on a strained Ag(100) surface, and find significantly enhanced rates for island diffusion and coarsening. © *1999 American Institute of Physics.* [S0021-9606(99)70135-2]

I. INTRODUCTION

The number of applications for epitaxial materials continues to increase, and with this increase has come more stringent requirements on the quality and properties of these materials. As a result, atomic-level control in the fabrication of nanostructures, *and* assessment of their stability, is becoming crucial. Surface science continues to confront this issue through studies of fundamental processes in the growth and equilibration of epitaxial films.[1] To gain the most complete picture of these processes, a common strategy is to begin by investigating less complex systems, one particularly simple example of which is metal(100) homoepitaxial thin films.

In the submonolayer regime, the key processes controlling homoepitaxial film growth and equilibration can be described as follows. During film growth, atoms adsorb irreversibly on the surface, then rapidly diffuse, colliding with each other to nucleate two-dimensional (2D) islands. Islands continue to grow in size as additional adatoms are incorporated. The ensemble of islands thus created on the surface constitutes a far-from-equilibrium state of the adlayer.[2] This state then undergoes post-deposition equilibration, during which the excess surface free energy associated with island edges is reduced by decreasing the number or density of islands, and thus increasing their mean size (that is by coarsening or ''ripening'' of the island distribution).

Traditionally, ''Ostwald ripening'' was believed to constitute the dominant kinetic pathway or mechanism for adlayer coarsening in homoepitaxial systems with 2D islands.[3] During Ostwald ripening, diffusion-mediated mass transport of adatoms (or vacancies) across terraces between 2D islands allows for the growth of large islands at the expense of small ones. Scanning tunneling microscopy (STM) studies have revealed that indeed Ostwald ripening dominates the coarsening of island distributions for Ag/Ag(111) at 295 K,[4] for Cu/Cu(111) between 300 and 355 K,[5] and for Cu/Cu(100) at 343 K.[6] In contrast, for Ag/Ag(100) and Cu/Cu(100) at 295 K, STM studies revealed that adlayer coarsening is typically dominated by the diffusion, and subsequent collision and coalescence of ''large'' 2D islands.[7,8] It is natural to describe this alternative coarsening mechanism as ''Smoluchowski ripening,'' recalling the long established and extensive use of Smoluchowski rate equations[9] to analyze various other diffusion-mediated coagulation processes.

The latter observations of Smoluchowski ripening on metal surfaces have motivated considerable interest in the process of diffusion of large 2D islands or clusters in its own right. Most studies to date have explored scaling relationships for the island diffusion coefficient, $D(s)$, versus island size, s, of the form $D(s) \approx D^* s^{-\alpha}$ (for sufficiently large s). Here, ''s'' denotes the number of atoms in the island, and D^* is a temperature-dependent prefactor which reflects the magnitude of the diffusion coefficient for islands of a few atoms. An early mean-field-type theoretical treatment[10] provided a direct (but over simplistic) relationship between the exponent, ''α,'' and the dominant atomistic mechanism underlying diffusion: $\alpha = \frac{3}{2}$ for ''perimeter diffusion'' (PD) in-

a)Electronic mail: evans@ameslab.gov

volving hopping of atoms along the island periphery; $\alpha=1$ for ''terrace diffusion'' (TD) involving correlated detachment and *re*attachment of atoms from the island perimeter (or diffusion of vacancies through the island); and $\alpha=\frac{1}{2}$ for ''evaporation and condensation'' (EC) involving uncorrelated detachment and attachment of atoms. However, pioneering simulation studied by Voter,[11] as well as more recent and extensive simulation studies,[12,13] and also recent theoretical[14] and experimental[8] investigations, have shown that these simple fractional values for α are not always realized. Nonetheless, it seems that larger exponent values still indicate that PD is dominant.

There is also a long history of analyses of processes involving coarsening of distributions of clusters on surfaces. Most have focused on Ostwald ripening,[3] although there were a number of studies particularly in the 1970's of Smoluchowski ripening for three-dimensional (3D) islands.[15–17] The latter, which are more closely related to this study, included analysis of not just mean island size, but also the evolution of the island size distribution including such features as its dispersion.[15,16] Related theoretical analyses employed mean-field Smoluchowski rate equations. More recent theoretical studies of Smoluchowski ripening have focused on arrays of 2D islands (motivated by the experimental studies mentioned above[7,8]), often employing kinetic Monte Carlo simulation to analyze suitable models, and thus avoiding the limitations of mean-field treatments.[18–20] The most sophisticated such studies[20] incorporate simulation results for island diffusivity, and have been generalized to allow for a competing Ostwald ripening pathway. One particularly simple but important relationship for Smoluchowski ripening follows from the mean-field analysis (and is confirmed in simulation studies): The temporal scaling exponent, β, for the mean island size, $s_{\mathrm{av}}\sim t^{\beta}$, is related to the size-scaling exponent, α, for cluster diffusivity by $\beta=1/(1+\alpha)$.[19] Here, s_{av} is measured in numbers of atoms, and the temporal scaling applies only for ''long'' times.

In this paper, we consider exclusively coarsening of 2D islands in the Ag/Ag(100) system at 295 K combining STM experiments with theoretical modeling. As noted above, diffusion of large 2D near-square clusters has been observed in this system, and coarsening is dominated by Smoluchowski ripening.[7] A comprehensive analysis of cluster diffusion, monitoring the relative position of roughly equal sized pairs of clusters, yielded an estimate of $\alpha=1.14$ with a chi-squared uncertainty of ± 0.05.[8] However, there is considerable scatter in the experimental data, an intrinsically large uncertainty in values for diffusivity, and additional uncertainty in island sizes. Thus, the uncertainty in α may be larger, and values up to at least 1.3 plausibly fit the data. Interestingly, observation of a single coarsening run over an extended period of about 28 hours yielded an estimate of $\beta\approx 0.466$,[8] consistent with $\alpha=1.14$. In this study, the rate of evaporation of adatoms from island edges was estimated independently and found to be sufficiently small that associated TD and EC mechanisms must be inoperative.[8] Thus, cluster diffusion was assumed to be dominated by PD in this system.

Another possibility was suggested in a recent simulation study of the diffusion of large 2D Cu clusters on Cu(100), which revealed a crossover with increasing island size from PD to TD mediated by *vacancy diffusion* through the cluster.[13] It was suggested that this behavior may be generally applicable for other metal(100) homoepitaxial systems, including Ag/Ag(100).[13] However, it has been noted that the relative dominance of PD versus vacancy TD will be strongly sensitive to the magnitude of rate for vacancy diffusion relative to the various PD rates, as well as to the cluster size.[21,22] From this perspective, the study in Ref. 13 might be somewhat biased towards vacancy TD, as it incorporates a very low choice of activation barrier for vacancy diffusion.[22–25] Thus, there is still some uncertainty as to the mechanism for diffusion of large Ag clusters on Ag(100).

A key experimental challenge in coalescence studies is to obtain sufficiently good statistics for a detailed quantitative analysis. Difficulty arises due to the intrinsically high fluctuations or ''noise'' in the underlying cluster diffusion and coalescence processes. (In this respect, Monte Carlo studies have an advantage in that noise is more easily assessed and reduced by extensive simulation trials.) One typically neglected problem in experimental studies of the coarsening kinetics is that there are strong temporal correlations, i.e., the number of islands always strictly decreases with time. A smooth decrease in island density with time hides the fact that a quite different behavior could result from repeating the experiment from the same initial island distribution (so, e.g., it is difficult to assess the uncertainty in β from a single run). Another problem is that despite the recent interest in island diffusion and coarsening in metal homoepitaxial systems, only limited and selective studies of coarsening kinetics have been performed. Consequently, in this study, we address these shortcomings by performing *tailored families of experiments*, wherein we systematically varying the initial value of the average island size by adjusting the amount of Ag deposited (up to 0.25 ML). The entire family of curves for average coarsening kinetics should vary smoothly (in fact, analytically), so deviations in experimental data from this trend reflect noise. Also, there is sufficient information in the variation of entire family of curves that one can directly assess size dependence of diffusivity. We also make use of a Smoluchowski rate equation to quantitatively relate the decrease in the mean island density to island diffusivity.

Analysis of island size distribution, and its evolution, is of course much more statistically demanding than analysis of just the mean size. The most extensive previous studies for Smoluchowski ripening have been for 3D islands, and have typically identified the natural increase in the mean size and associated broadening of the distribution during coarsening.[3] Related theoretical studies invariably focus on the asymptotic evolution and shape selection.[26] However, little effort has been made to assess the evolution in the intrinsic shape of island size distribution, as characterized by the appropriate scaling function. This transient behavior is of particular experimental relevance, as the asymptotic regime may not be accessible, and as it allows assessment of the extent of the early changes occurring before the first STM observation. The latter is crucial in order to correctly surmise the ''initial'' post-deposition form of the size distribution for appropriate comparison with predictions of nucleation theory. (In

fact, the form produced by the nucleation and growth process has only been understood very recently.[27–29]) Thus, we characterize the initial shape evolution in this paper. To this end, we find it instructive to consider the variance of the scaling function (as opposed to the dispersion of the size distribution considered previously,[15,16] the behavior of which is driven by the increase in the mean island size). Reasonably accurate experimental determination of this variance is viable, in contrast to the full shape of the size distribution.

Finally, we report experimental data revealing that surface strain can have a strong influence on island diffusion and thus Smoluchowski ripening on larger terraces. This observation implies that some care should be taken an interpreting data for nominally unstrained surfaces.

II. EXPERIMENTAL DETAILS

Scanning tunneling microscopy has become the technique of choice for performing studies of island diffusion and adlayer coarsening in homoepitaxial metal adlayers. Its inherent ability to image the metal surface with unparalleled resolution, and to record real-time changes in ensembles of 2D islands, makes it the ideal tool for investigating such processes. Our experimental data are acquired using an Omicron room temperature STM housed in an ultra-high vacuum chamber with a base pressure of 6×10^{-11} to 2×10^{-10} Torr. The Ag(100) substrate is prepared through cycles of Ar ion sputtering and annealing to 700 K. Contamination is minimal, based inspection of STM images and Auger spectroscopy. Silver is deposited on the substrate from a home-built, liquid-nitrogen-shrouded source, with the substrate temperature always held at 295 K. However, the deposition flux and deposition time can be adjusted to yield various coverages, and initial values for the mean island density or size.

After deposition, the first STM image is typically obtained within 25–50 min. It should be noted that the island density can be significantly reduced (by 5%–15%) due to coarsening before this image is taken.[30,31] The subsequent time evolution of the system, discussed in detail in the following sections, is monitored at a rate to 2 to 3 min/frame. The tunneling parameters employed (voltage=0.7–1.5 V, current=0.3–0.5 nA) have been determined previously to minimize the STM tip–surface interaction.[7,31] The island density and size distribution data in our analysis are obtained from the central portions of terraces wider than 1500 Å in order to minimize the effects of step edges on island distributions.

III. EXPERIMENTAL RESULTS AND DISCUSSION

In the following discussion, $a=2.89$ Å denote the surface lattice constant for Ag(100). Also, θ denotes the time-invariant post-deposition coverage (measured in monolayers), $N_{\rm av}$ denotes the mean island density (measured in units of islands per adsorption site), $L_{\rm av}$ denotes the mean separation of island centers (measured in units of distance), and $s_{\rm av}$ denotes the mean island size (measured in units of atoms). These quantities are simply related by

$$L_{\rm av}=a(N_{\rm av})^{-12} \text{ and } s_{\rm av}=\theta/N_{\rm av}. \quad (1)$$

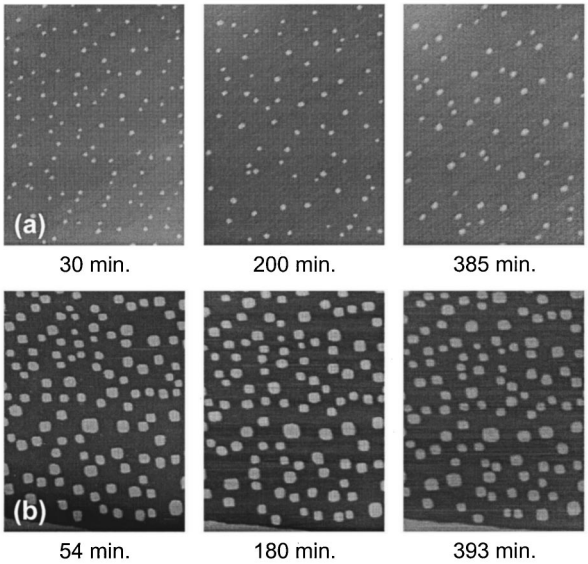

FIG. 1. Sequences of STM images of the ripening of Ag island distributions on Ag(100) for two coverages: (a) $\theta=0.02$ ML, with $s^0_{\rm av}=60$ atoms; (b) $\beta=0.21$ ML with $s^0_{\rm av}=510$ atoms. All images are 150 nm×100 nm.

Thus, $N_{\rm av}$ will decrease in time during coarsening, and both $L_{\rm av}$ and $s_{\rm av}$ will increase in time, from their initial post-deposition values, which we denote by $N^0_{\rm av}$, $L^0_{\rm av}$, and $s^0_{\rm av}$, respectively.

Typical sequences of STM images from two coarsening experiments are shown in Figs. 1(a) and 1(b) for initial values, $s^0_{\rm av}$, of the mean island sizes of 60 and 510 atoms, respectively. Both the general nature of evolution in these images, and the specific feature that ripening is more rapid in the case with smaller $s^0_{\rm av}$, are consistent with the traditional perception that Ostwald ripening should dominate coarsening in metal homoepitaxial systems.[3] However, a detailed examination of the coarsening process, utilizing all of the experimental images, reveals that the contribution from Ostwald ripening is negligible, lying within the experimental noise. Instead, island diffusion, and subsequent collision and coalescence (or Smoluchowski ripening) produce essentially all of the coarsening.[7] This conclusion is supported by independent studies for Ag/Ag(100) and Cu/Cu(100) at 295 K.[8]

In order to most effectively assess whether island diffusion rates are size-dependent, it is natural to create initial island distributions with roughly fixed island separations, $L^0_{\rm av}$, and varying mean island sizes, $s^0_{\rm av}$. This is readily achieved noting a basic result from nucleation theory that the mean island density, $N^0_{\rm av}$, is largely independent of coverage between 0.05 and 0.25 ML.[2] More specifically, for irreversible island formation at fixed temperature, one has[2]

$$N^0_{\rm av}\sim F^{1/3}, \text{ so } L^0_{\rm av}\sim aF^{-1/6}, \text{ and } s^0_{\rm av}\sim \theta F^{-1/3}. \quad (2)$$

This regime applies for Ag deposition on Ag(100) below about 310 K, and thus at 295 K.[31] Thus, by depositing various amounts of Ag, at approximately *constant flux*, F, we maintain a roughly constant $N^0_{\rm av}$ and $L^0_{\rm av}$, but can control the initial value of the mean island size, $s^0_{\rm av}$. Specifically, $s^0_{\rm av}$ varies roughly linearly with submonolayer coverage, θ, which in turn varies linearly with deposition time (for fixed

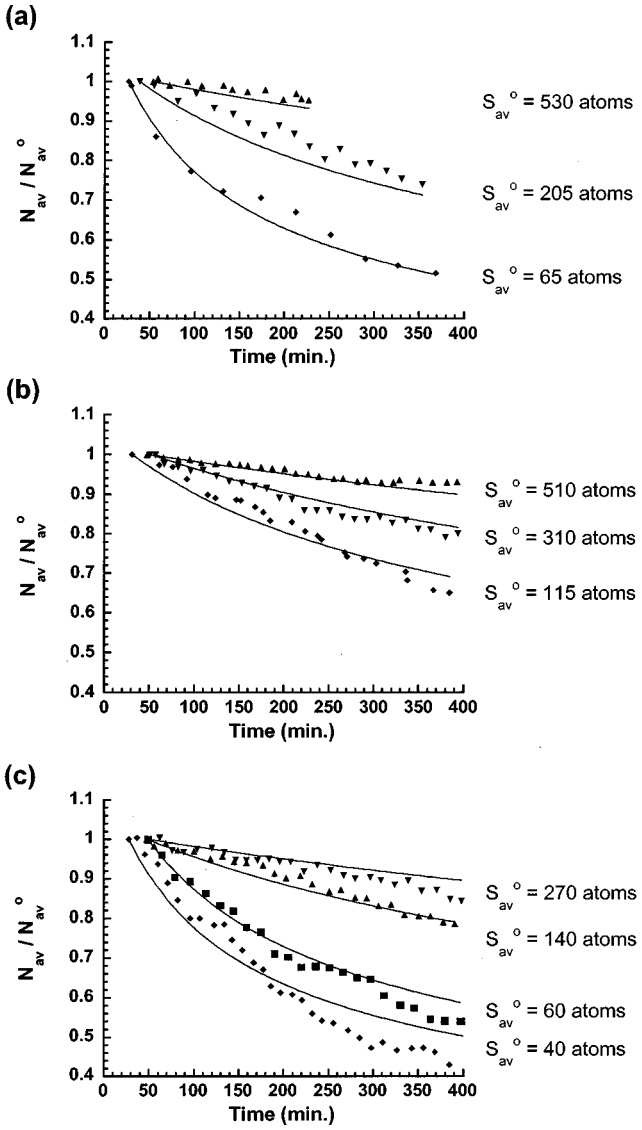

FIG. 2. Families of data illustrating the coarsening kinetics for three different fluxes: (a) $F=0.011$ ML/s; (b) $F=0.006$ ML/s; (c) $F=0.003$ ML/s. Data points for each STM experiment are shown as various solid symbols labeled by s_{av}^0-values. Corresponding behavior predicted from Eq. (8) with $\alpha=1.5$ and $D_0=50$ Å^2/s is shown as solid curves.

F). In fact, by depositing between 0.01 and 0.25 ML, we can readily access a broad range of initial values for s_{av}^0.

Each ensemble of islands thus created was then monitored at roughly periodic intervals to determine the decrease of island density, N_{av}, with time, thus generating a coarsening curve characteristic of a specific value of s_{av}^0 (and of L_{av}^0). We plot families of such coarsesning curves for varying s_{av}^0 (and roughly fixed L_{av}^0). In fact, Fig. 2 shows three such families of curves (each family corresponding to a different value of F or L_{av}^0). The values of s_{av}^0, θ, N_{av}^0, and the actual initial number of islands observed, are summarized in TableI.

Based on the trends within each family of coarsening curves in Fig. 2, we can immediately assess the variation of cluster diffusion coefficient, $D(s)$, with size, s. By increasing s_{av}^0 (or θ), with fixed island center–center separation, L_{av}^0, the average separation between *island edges* is reduced, shortening the distance for islands to diffuse before coalescing. Thus, if $D(s)$ were completely independent of s, the rate of coarsening should actually *increase* with increasing s_{av}^0 (or θ), due to this shorter distance. In contrast, the *opposite* behavior is observed in Fig. 2, where the coarsening rate *decreases* strongly with increasing s_{av}^0 (or θ). This can only be ascribed to a strong decrease in $D(s)$ with increasing s. A more detailed analysis is presented in Sec. IV.

TABLE I. Summary of initial conditions for the three families of data for coarsening kinetics shown in Fig. 2. Shown are values for s_{av}^0, θ, N_{av}^0, and the initial value of the total number of islands in the region analyzed.

(a) Flux=0.011 ML/s S_{av}^0(atoms/island)	θ(% ML)	$N_{av}^0\times10^{-5}$ (Å^{-2})	Number of islands
530	25	5.7	230
205	14	8.1	165
65	4	7.3	145
(b) Flux=0.006 ML/s S_{av}^0(atoms/island)	θ(% ML)	$N_{av}^0\times10^{-5}$(Å^{-2})	Number of islands
510	21	4.9	278
310	16	6.2	296
115	5	5.2	248
(c) Flux=0.003 ML/s S_{av}^0 (atoms/island)	θ(% ML)	$N_{av}^0\times10^{-5}$ (Å^{-2})	Number of islands
270	8	3.5	123
140	5	4.2	150
60	2	4.0	109
40	1	3.1	140

Finally, we mention one significant issue pertinent for modeling data particularly for smaller island sizes or coverages. STM tip scans may have a tendency to disproportionately magnify small features.[32] This can result in an overestimation of θ (and thus s_{av}^0), so it is important to try to correct for this effect before detailed comparison between theory and experiment. Of course, the inherently low resolution in STM caused by scanning large surface areas also produces larger uncertainty in θ and s_{av}^0 values for small adlayer coverages.

IV. THEORETICAL ANALYSIS OF EVOLUTION OF THE MEAN ISLAND DENSITY

The Smoluchowski rate equation approach,[9] first advanced over 80 years ago, has been employed widely to describe the kinetics of coagulation, aggregation, reaction, and coarsening. As noted in Sec. I, this approach has been applied extensively to analyze the Smoluchowski ripening of 3D clusters on surfaces,[15–17] but relatively little work has been done for 2D clusters. Thus, in this section, we present these standard mean-field rate equations, together with a minor refinement, in order to analyze the coarsening data of Sec. III.

Extending the notation introduced in Sec. III, we let N_s denote the density (per adsorption site) of islands of s atoms. Then, the mean-field Smoluchowski rate equations for these island densities have the generic form[9,15–19]

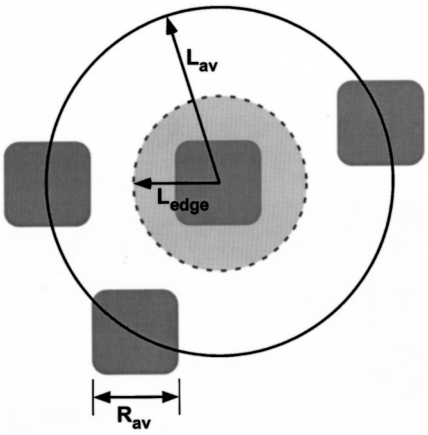

FIG. 3. Schematic showing the key linear dimensions for a typical island distribution: The mean separation between island centers, $L_{av}=(N_{av})^{-1/2}$; the mean island edge length, $R_{av}=\theta^{1/2}L_{av}$; and the mean separation between island edges, $L_{edge}=L_{av}-cR_{av}=(1-c\,\theta^{1/2})L_{av}$, where c is of order unity.

$$d/dt\ N_s=\tfrac{1}{2}\sum_{s'+s''=s} K(s',s'')N_{s'}N_{s''}-\Sigma_{s'}K(s,s')N_sN_{s'}, \tag{3}$$

where $K(s,s')$ describes the rate of collisions between islands of size s and s'. Assuming that this rate has the form $K(s,s')=k(s)+k(s')$, these equations can be contracted to an equation for the mean island density (per adsorption site), $N_{av}=\Sigma_s N_s$, of the form

$$d/dt\ N_{av}=-N_{av}/\tau, \text{ where } 1/\tau=\Sigma_s k(s)N_s=k_{av}N_{av}. \tag{4}$$

Here, τ corresponds to the typical lifetime of a diffusing island, and we have defined $k_{av}=\Sigma_s k(s)N_s/N_{av}$. Equation (4) is not closed (without further approximation), but rather represents the first in a hierarchy of equations for various moments of N_s (see Appendix A). Usually, $k(s)$ is related to the diffusion coefficient for islands of size s, often invoking a detailed analysis of diffusion-mediated aggregation.[9,33] Then τ is inversely proportional to some mean diffusivity. Given the limitations of even sophisticated mean-field treatments of capture (see below), we prefer a simpler treatment which accounts for the often neglected (but important) feature that the linear dimension of coalescing islands is often a significant fraction of their separation. By so doing, we directly reveal the strong dependence of τ on θ, in addition to its dependence on the mean island diffusivity.

First, we observe that for 2D near-square islands, the mean separation between island edges (see Fig. 3) has the form $L_{edge}=(1-c\,\theta^{1/2})L_{av}$, where the geometrical factor, c, is determined by the details of the island distribution. It will be approximated by unity in our analysis below. Then, for a diffusing island to reach another island, we note that it typically needs only travel a net distance L_{edge}, rather than the longer distance L_{av}. Thus, according to the Einstein relation, one has[7,34,35]

$$(L_{edge})^2\approx 2(4D_{av})\tau. \tag{5}$$

Here, D_{av} denotes the mean island diffusivity, and the factor of 2 outside the parentheses arises since both islands involved the coalescence event are mobile. Solving this equation for the lifetime, τ, and substituting into Eq. (4), reveals that[34]

$$d/dt\ N_{av}=-8a^{-2}D_{av}(1-c\,\theta^{1/2})^{-2}(N_{av})^2. \tag{6}$$

A simple correspondence with the Smoluchowski equations [Eq. (3)] can be made by assigning $k(s)=8D(s)(1-c\,\theta^{1/2})^{-2}$. However, a more precise form for $k(s)$ would be based on an estimate the typical separation between the edge of an island size s and other those of islands (rather than just on the average, L_{edge}). Below, we adopt the further approximation

$$D_{av}=\sum_s D(s)N_s/N_{av}\approx D(s_{av}), \tag{7}$$

where

$$s_{av}=\sum_s sN_s/N_{av}=\theta/N_{av},$$

which becomes precise for narrow island size distributions. See Appendix A. From the assumed form, $D(s)\approx D^*s^{-\alpha}$, one obtains $D_{av}\approx D^*\theta^{\alpha}(N_{av})^{-\alpha}$. Then, substitution into Eq. (6) and integration yields

$$N_{av}\approx[(N_{av}^0)^{-1/\beta}+(1+\alpha)At]^{-\beta}, \text{ where } \beta=1/(1+\alpha), \tag{8}$$

and where $A=8(a)^{-2}D^*\theta^{-\alpha}(1-\theta^{-1/2})^{-2}$, and again N_{av}^0 is the initial island density.

The experimental coarsening data presented in Sec. III can be reasonably fit by choosing $\alpha\approx 1.5$, with a corresponding $D^*\approx 50$ Å^2/s. The coarsening curves generated from Eq. (8) for these parameters are shown as solid lines in Figs. 2(a)–2(c). Figure 4 provides some assessment of the sensitivity of the fit by showing rate equation curves with

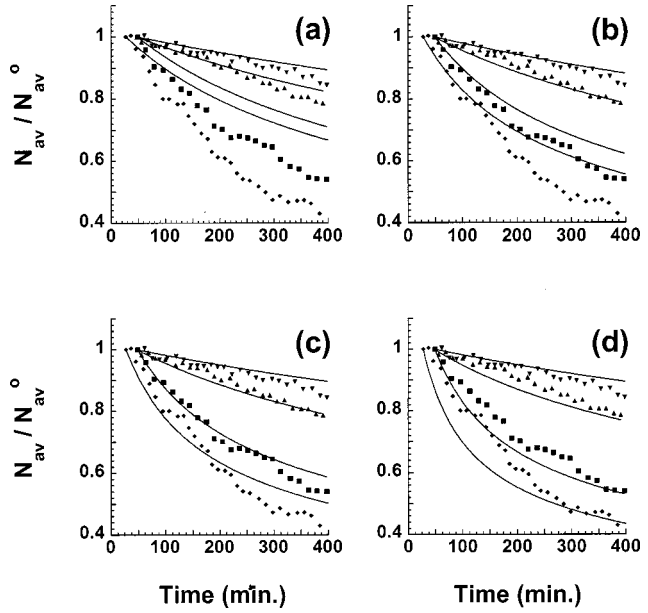

FIG. 4. Best fits to the family of data for the experimental coarsening kinetics with $F=0.003$ ML/s [Fig. 2(c)] from the rate equations with various $\alpha=1.0$ (a); 1.25 (b); 1.5 (c); 1.75 (d). Solid symbols show experimental data, and solid curves show predictions from Eq. (8).

α-values of 1.0, 1.25, 1.5, and 1.75, for one family of experimental coarsening curves. Fits for $\alpha=1.5$ and 1.75 are comparable, but the smaller values of 1.25 seems to produce too weak a s-dependence to $D(s)$ to describe the dramatic increase in coarsening rates upon decreasing s_{av}^0 to 40 atoms. However, the uncertainties in estimates of θ and s_{av}^0 are greaest for small cluster sizes. Also, as noted in Sec. I, the magnitude of the noise or uncertainty in the experimental data is hidden by strong temporal correlations in N_{av} in each coarsening experiment. Thus, the uncertainty in our estimate of $\alpha\approx1.5$ is substantial, perhaps ±0.25. This α-value is larger than the previously reported value of $\alpha=1.14$ (and a corresponding $D^*=18.5$ Å^2/s),[8] but there is no clear inconsistency given the substantial uncertainties (see also Sec. I). We plan a subsequent analysis of these coarsening processes using Monte Carlo simulation, which will elucidate the intrinsic noise in the coarsening process, and thus allow better assessment of uncertainties in α-estimates. These simulations will also account for spatial correlations in the island distribution, which are ignored in the rate equation approach.

Finally, we comment briefly on our previous modeling of coarsening data. In Ref. 7, we neglected the size dependence of island diffusivity, but accounted for coverage dependence of the lifetime τ. A reasonable fit to coarsening data was obtained because we only compared situations with similar mean island size (and thus D_{av}), but differing mean island separations.

V. EVOLUTION OF THE SHAPE OF THE ISLAND SIZE DISTRIBUTION

It is common to express the island densities, N_s, in the scaled from[27,28]

$$N_s\approx\theta(s_{av})^{-2}f(s/s_{av},t) \text{ for large } s_{av}. \tag{9}$$

Then, the scaling function ''f'' describing the *shape* of the island size distribution satisfies

$$\int_0^\infty f(x,t)dx=\int_0^\infty xf(x,t)dx=1,$$

and

$$\int_0^\infty (x-1)^2f(x,t)dx=\sigma(t)^2, \tag{10}$$

where $\sigma(t)$ denotes the standard deviation or width of the scaling function. The first two normalization conditions follow from the constraints $\Sigma_s N_s=N_{av}$, and $\Sigma_s sN_s=\theta$. In Eq. (10), we also use $x=s/s_{av}$ to denote the natural scaled island size variable.

There have been extensive studies[2] of the initial shape of the size distribution, $f(x,0)=f_0(x)$, produced by the nucleation and growth process, although its form was only recently understood.[28,29] Such distributions have a significant population of small islands (compared with the average size),[27] particularly for irreversible island formation, which applies for the Ag/Ag(100) system at room temperature.[31] Separate theoretical studies of coarsening have demonstrated that a distinct shape, determined by the details of the coarsening process, is selected for long times.[3,19,26] In particular, for Smoluchowski ripening, this selected shape is determined by the size-dependence of cluster diffusivity. See Refs. 19, 26, and Appendix B. Here, we are naturally interested in the evolution of $f(x,t)$ from the form $f_0(x)$ induced by cluster diffusion and coalescence with the observed strongly size-dependent cluster diffusivity. Intuitively, one expects a rapid initial depletion of these smaller islands, due to their higher mobility, and thus an associated rapid and significant change in shape of $f(x,t)$.

From the experimental perspective, there are two key challenges with analyzing the island size distribution. First, as noted in Sec. II, a significant period of time elapses after deposition ceases and before the first STM image is acquired, so any rapid changes may not be seen. Second, as noted in Sec. I, typically one cannot obtain sufficient data to reduce the intrinsic statistical noise to the extent needed to allow accurate determination of the shape of the island size distribution (or its evolution). Because of the latter, our experimental analysis focused on evolution of the width, $\sigma(t)$, of the scaling function.

To quantify the evolution of the island size distribution, and of $\sigma(t)$ in particular, we integrate the Smoluchowski equations [Eq. (3)] for the island densities, N_s, and from the results extract $f(x,t)$. For a more direct analysis of the evolution of $f(x,t)$, see Appendix B. We assign cluster collision rates consistent with cluster diffusivity $D(s)=D^*s^{-\alpha}$, choosing $\alpha=1.5$ and $D^*=50$ Å^2/s, and select an initial size distribution based on nucleation theory, as now discussed in more detail. For Ag/Ag(100), experimental data suggests that the formation of near-square islands is effectively irreversibly at 295 K, and that cluster diffusion does not play a significant role *during* this process.[31] Simulations appropriate for this scenario show that $f_0(x)$ has the characteristic monomodal form: It has a maximum value at $x=x_{max}\approx1.1$ of $f_0(x_{max})\approx0.78$, decreasing to a minimum of about 0.30 at x decreases to $x\approx0.02$ (before increasing slightly at $x=0$), and a variance of $\sigma^2\approx0.24$.[29] With this initial distribution, we find that the variance, $\sigma(t)^2$, at first decreases slightly (to just below 0.2) before slowly increasing. However, we shall see below that experimentally observed minimum values for σ^2 are around 0.1, but with a *large uncertainty* (cf. Appendix C). This suggests some modification of the above choice of initial size distribution is appropriate. Previous studies have shown that some mobility of dimers and other small clusters during deposition can significantly modify this distribution, without affecting the scaling of N_{av}.[36] Specifically, small cluster mobility reduces $f_0(0)$, increases $f_0(x_{max})$, and produces more rapid decay of $f(x)$ for x above x_{max}, thus reducing σ^2. (The onset of reversibility during island nucleation has the same effect.[31,37]) Such a modified choice of $f_0(x)$ with $\sigma^2\approx0.18$ is used below.

Figure 5(a) shows the results for the evolution of $f(x,t)$, choosing an initial $f_0(x)$ as described above, and choosing $\theta=0.16$ ML and $N_{av}^0=5.1\times10^{-4}$/site (so $s_{av}^0\approx315$ atoms). We find significant evolution of $f(x,t)$ from the initial form $f_0(x,t)$ in the first several minutes, with a somewhat narrower form depleted of small islands being achieved after only about $\frac{1}{2}$–$\frac{3}{4}$ of an hour. This latter form [highlighted in Fig. 6(a) at 50 min] is consistent with experimental data in

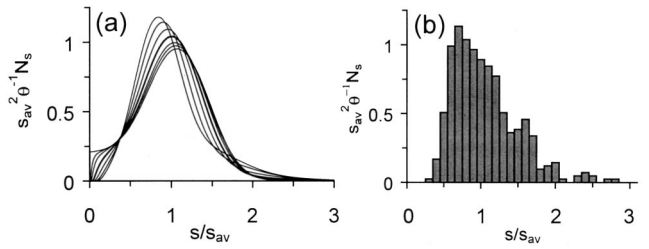

FIG. 5. (a) Rate equation prediction for the evolution of the shape, $f(x,t)$, of the island size distribution using an initial form, $f_0(x)$, with a variance of 0.18 as described in the text. We set $\theta=0.16$ ML and $s_{av}^0=315$ atoms. Curves show the form for the following times measured after deposition: 0 min (the initial form), 5, 15, 50 (darker curve), 120, 240, and 400 min. As time increases, the left shoulder on the curve decreases, the peak increases, the right flank moves toward the left, and the large-x tail increases. (b) The experimental size distribution from images containing a total of 420 islands [with $s_{av}^0=315$ atoms as in (a)] obtained about 50 min after deposition of $\theta\approx0.16$ ML of Ag at 295 K with a flux $F\approx0.006$ ML/s.

Fig. 5(b) obtained from analysis of STM images of island distributions (with 420 islands) on broad terraces with the same θ and N_{av}^0 obtained about 50 min after deposition. An important conclusion from this study is that caution is necessary when comparing experimental island distributions measured ''just after'' deposition with theoretical predictions from nucleation theory.[31] Even in the ''short'' time required to obtain the first STM image, there can be significant evolution of the size distribution away from its initial post-deposition form.

Finally, in Fig. 6, we compare experimental observations and corresponding rate equation predictions for the evolution of $\sigma(t)^2$ for three cases with $F=0.003$ ML/s and $\theta=0.02$, 0.05, and 0.08 ML (see Table I c). The initial values for s_{av}^0 in the rate equation analysis are chosen as 55, 138, 268 atoms to recover reported experimental values at the initial observation time (of around 50 min) of 60, 140, and 270 atoms, respectively. The rate equation predictions reveal an *initial decrease* from our chosen initial value of $\sigma^2=0.18$ to about 0.16, followed by a much slower increase. Given the substantial experimental uncertainties in estimating σ^2-values (see Appendix C), overall behavior is consistent with experimental observations (where an initial decrease presumably occurs before the first data point). The consistent slow increase in σ^2 for longer times reflects the gradual development of a ''slowly decaying tail'' on the distribution for large x. This feature is characteristic of the asymptotic long-time form, $f_\infty(x)$, which has a substantially larger value of σ^2 than does $f_0(x)$. See Appendix B.

VI. SURFACE STRAIN AND ITS INFLUENCE ON ISLAND DIFFUSION AND COARSENING

The effect of surface strain on adsorbate diffusion and crystal growth continues to attract interest. Long ago, Bauer developed thermodynamic criteria for near-equilibrium heteroepitaxial film configurations, where strain occurs due to lattice mismatch.[38] However, more recent studies have considered situations where heteroepitaxial growth is dominated by kinetics.[39] In homoepitaxial systems, one inevitably encounters surface strain induced by defects and dislocations. Can the resulting stresses affect the kinetics of surface processes? In Fig. 7, an STM image is shown following the deposition of 0.18 ML of Ag on Ag(100) producing a distribution of large islands with $s_{av}^0\approx490$ atoms. In the center of the image is a strained, oblong-shaped region, with a maximum height of ~0.7 Å above the unstrained portion of the surface. The origin of the strain is undetermined. The coarsening kinetics for islands around this region is displayed in Fig. 8. The central observation is that the coarsening is much faster than predicted by mean-field rate equations of Sec. III with $\alpha=1.5$ and $D^*=50$ Å^2/s (dashed line in Fig. 8). The observed coarsening can be reasonably described by rate equations using $D^*=250$ Å^2/s, keeping $\alpha=1.5$ (solid line in Fig. 8). This fivefold increase in D^* produces a corresponding increase in the coarsening rate of roughly five times. Note that the choice $\alpha=1.5$ is maintained for simplicity, but a different size dependence from unstrained adlayers is quite plausible (see below). One conclusion from these observations is that undetected strain could ''corrupt'' experimental estimation of $D(s)$ versus s for nominally unstrained surfaces.

To elucidate our observations, we apply some ideas developed in recent analyses of the role of surface strain in heteroepitaxial film growth. In studies of the formation of

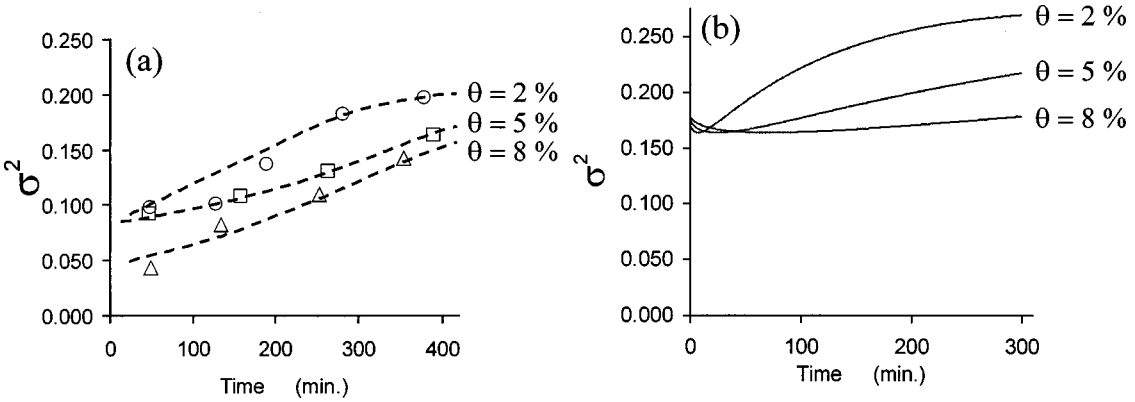

FIG. 6. Evolution of the variance, σ^2, for three cases corresponding to experiments with $F=0.003$ ML/s and coverages of 0.02, 0.05, and 0.08 ML. (a) Estimates from experimental data (symbols), where dashed lines are shown as a guide to the general trend. (b) Rate equation predictions using an initial shape for the island size distribution, $f_0(x)$, with a variance of 0.18, as described in the text, and using θ- and s_{av}^0-values consistent with experiment.

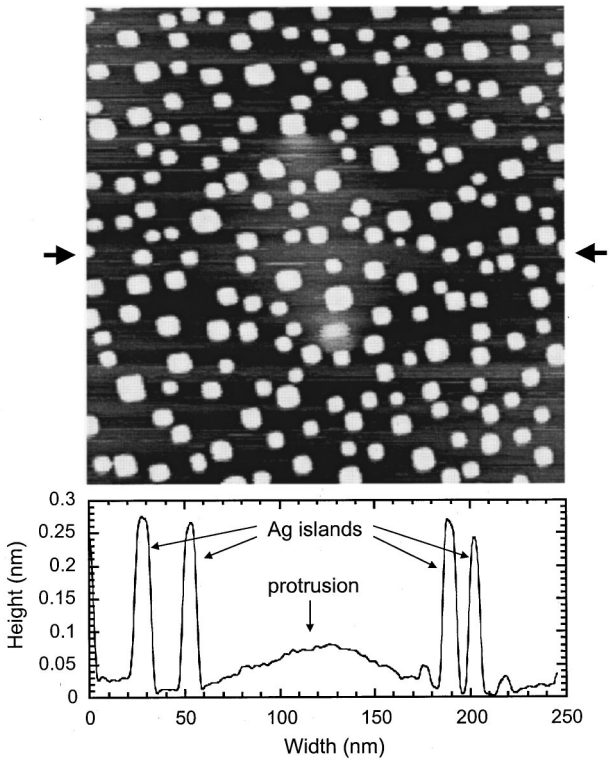

FIG. 7. Top: STM image of a 250 nm×250 nm region showing 0.18 ML of Ag deposited on Ag(100). Bottom: Cross-sectional height profile taken horizontally through the center of the image (at a level indicated by the arrows), and spanning the oblong-shaped central protrusion.

strained islands, it was proposed that the barrier for adatom detachment or dissociation from island edges, E_{DISS}, should be reduced by the strain energy per adatom of the island.[40] This strain energy/atom increases with island size. We relate these observations to PD-mediated cluster diffusion as follows. Barriers for detachment, E_{DISS}, are roughly given by the sum of the terrace diffusion barrier, E_d, plus a multiple of an effective nearest-neighbor interaction, J; those for perimeter diffusion, E_{PD}, are the sum of the barrier for diffusion along close-packed ⟨110⟩ edges, $E_e \approx E_d/2$, plus a multiple of J.[22,23] A strain-induced reduction of E_{DISS} suggests a reduction in J, and thus a reduction in E_{PD} (although other behavior is possible[41]). As a result, rates for cluster diffusion via the PD mechanism should be enhanced by strain, the effect being greater for large islands as in Fig. 7 where $s_{\mathrm{av}}^0 \approx 490$ atoms. Considering the possibility that cluster diffusion is mediated by TD of vacancies, tensile strain (as expected here) tends to raise barriers for adatom diffusion.[41,42] However, it might lower barriers for vacancy diffusion, which would be needed for consistency with observed behavior.

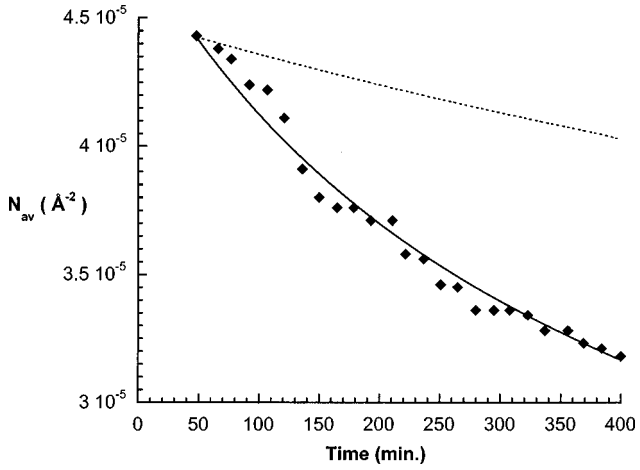

FIG. 8. Experimental data (solid symbols) for the coarsening kinetics for the region displayed in Fig. 7. Rate equations with the modified choice of parameters $D_0 = 250$ Å^2/s and $\alpha = 1.5$ (solid curve) fit observed behavior, in contrast to those with the previous choice $D_0 = 50$ Å^2/s and $\alpha = 1.5$ (dashed curve).

The general scenario of strain-enhanced cluster diffusion is also supported by a study of the motion of large vacancy clusters on Cu(111) surfaces, which found enhanced cluster diffusion upon addition of submonolayer amounts of Co.[43] This effect was attributed to the creation of local strain fields resulting from the substitution of Co with the top layer of Cu. Finally, we note that other novel mechanisms have been proposed to mediate the diffusion of strained heteroepitaxial islands, e.g., the formation of misfit dislocations separating portions of islands with adatoms occupying fcc (face-centered-cubic) and hcp (hexagonal-close-packed) sites on (111) surfaces.[44] Novel mechanisms may also operate for strained island diffusion on (100) surfaces.

VII. CONCLUSIONS

In summary, we have performed tailored experiments of the coarsening of 2D Ag island distributions on Ag(100). Coarsening is dominated by cluster diffusion and coalescence at 295 K. The coarsening kinetics show that the island diffusion coefficients must decrease strongly with size for clusters with tens to hundreds of atoms. Analyzing experimental data with an appropriate mean-field rate equation suggests a size scaling exponent of $\alpha \approx 1.5$. Given this characterization of cluster diffusivity, we also use mean-field rate equations to assess the rapid initial evolution in the shape of the island size distribution, and the evolution over longer times of the width of the scaling function for the size distribution. Since these rate equations do not account for spatial correlations in the island distribution, or elucidate the intrinsic noise or uncertainty in the experimental data for coarsening of finite ensembles of a few hundred (or less) islands, we plan to assess these issues in a future kinetic Monte Carlo simulation study. Finally, we analyzed coarsening behavior on a strained surfaced, showing that surface stresses can result in significantly increased cluster diffusion and coarsening rates.

ACKNOWLEDGMENTS

We would like to thank Maria Bartelt for useful discussions. This work was supported by NSF Grant No. CHE-9700592, and by the Institute of Physical Research and Technology (IPRT) at Iowa State University. It was performed at Ames Laboratory, which is operated for the U.S. Department of Energy by Iowa State University under Contract No. W-7405-Eng-82.

APPENDIX A: EVOLUTION OF THE MOMENTS OF THE ISLAND SIZE DISTRIBUTION

Statistical limitations often preclude reliable experimental determination of the island size distribution, $N_s \approx \theta(s_{av})^2 f(s/s_{av},t)$ versus s. Thus, it is natural to instead consider the moments

$$M_j = \sum_s s^j N_s \approx N_{av}(s_{av})^j \int_0^\infty dx\ x^j f(x,t), \tag{A1}$$

or related quantities. For example, one has $N_{av}=M_0, \theta = M_1$, and $\sigma^2 = M_2 M_0 (M_1)^{-2} - 1$. For this reason, we note that a direct description of the evolution of the M_j is possible. Assuming that $K(s,s')=k(s)+k(s')$ and defining $K_j = \Sigma_s s^j k(s) N_s$, from the Smoluchowski equations [Eq. (3)] one has

$$\begin{aligned} &d/dt\ M_0 = -K_0 M_0, \quad d/dt\ M_1 = 0, \quad d/dt\ M_2 = 2K_1 M_1, \\ &d/dt\ M_3 = 4K_3 M_1 + 6K_2 M_2 + 4K_1 M_3, \ldots . \end{aligned} \tag{A2}$$

An analysis might proceed by expressing the K_j in terms of the moments, M_j, or in terms of related quantities. To this end, a Taylor expansion, $k(s)=k(s_{av})+(s-s_{av})k'(s_{av})+$, can be utilized to obtain, e.g., $k_{av}=K_0/M_0=k(s_{av}) + \frac{1}{2}(s_{av})^2\sigma^2 k''(s_{av})+\cdots$. See Ref. 16 for a different approach.

In the lowest-order approximation, $k_{av}\approx k(s_{av})$ [cf. Eq. (8)], one obtains $d/dt\ M_0 \approx -k(s_{av})(M_0)^2$. One can readily develop more accurate higher-order approximations for narrow island size distributions (with $\sigma \ll 1$), but this task is more difficult for broader distributions. For the choice $k(s) \propto s^{-\alpha}$, the error in the lowest-order approximation for large s_{av} can be assessed from the relation $k_{av}=R(t)\cdot k(s_{av})$, where $R(t)=\int_0^\infty x^{-\alpha} f(x,t)dx$. In the notation of Sec. IV, this corresponds to $D_{av}=R(t)\cdot D(s_{av})$, and an approximation is used in Eqs. (8) and (9) replacing R by unity.

APPENDIX B: EVOLUTION OF THE SHAPE OF THE ISLAND SIZE DISTRIBUTION

In the regime of large s_{av}, one can reasonably replace the discrete variable, s, by a continuous variable, and rewrite the Smoluchowski equations with $K(s,s')=k(s)+k(s')$ as

$$\begin{aligned} d/dt\ N_s \approx &\frac{1}{2}\int_0^s ds'[k(s')+k(s-s')]N_s N_{s-s'} \\ &- \int_0^\infty [k(s)+k(s')]N_s N_{s'}. \end{aligned} \tag{B1}$$

We assume that $k(s)\propto s^{-\alpha}$, and thus can write $k(s) = k(s_{av})(s/s_{av})^{-\alpha}$. Using $N_s \approx \theta(s_{av})^2 f(s/s_{av},t)$, we extract from Eq. (B1) an equation for f in terms of the variable $x = s/s_{av}$. The left-hand-side (lhs) of Eq. (B1) becomes

$$d/dt\ N_s = \theta(s_{av})^{-2}[(d/dt(\ln s_{av})(-2f - x\cdot f_x) + f_t], \tag{B2}$$

and we note that

$$d/dt(\ln s_{av}) = -d/dt(\ln N_{av}) = R\cdot k(s_{av}) N_{av} = 1/\tau. \tag{B3}$$

Similar analysis of the right-hand-side (rhs) of Eq. (B1) yields an integro-partial differential equation for evolution of $f(x,t)$ which has the form

$$\begin{aligned} &\tau\partial/\partial t\ f - x\partial/\partial x\ f - 2f \\ &= R^{-1}\left\{\frac{1}{2}\int_0^x dx'[(x')^\alpha + (x-x')^{-\alpha}]f(x',t)f(x-x',t) \right. \\ &\quad \left. - \int_0^\infty dx'[(x)^{-\alpha} + (x')^{-\alpha}]f(x,t)f(x',t)\right\}, \end{aligned} \tag{B4}$$

where $R=\int_0^\infty x^{-\alpha} f(x,t)dx$, as in Appendix A. Evolution via Eq. (B4) ensures that both $\int_0^\infty dx\ f(x,t)$ and $\int_0^\infty dx\ x f(x,t)$ are time-invariant (and thus remain equal to their initial values of unity).

Note that an analogous equation is aqvailable for the initial form, $f_0(x)$, of $f(x,t)$.[28] Also, the time-invariant version of Eq. (B4) was obtained by Kandel[26] (apart from a typographical error). It is clear from Eq. (B4) that the long-time limit, $f_\infty(x)$, of $f(x,t)$ is determined by α. An often quoted asymptotic estimate is[19] $f_\infty(x)\sim x^\alpha \exp[-(\alpha+1)x]$, for which $\sigma^2=0.4$ when $\alpha=1.5$.

APPENDIX C: UNCERTAINTY IN EXPERIMENTAL ESTIMATION OF SIZE DISTRIBUTION PROPERTIES

In analyzing experimental data, we estimate properties of the island size distribution from finite samples of M islands, where $M\approx 100$–300. Thus, it is appropriate to assess the expected values and likely error in these estimates. Below we let $E[X]$ denote the expected value of some measured quantity X, and $V[X]$ its mean-square uncertainty or variance. The ''standard error'' in the estimate is just the square root of this variance. Here, we neglect spatial correlations in the island distribution. Of obvious interest is the estimate, $s_{av}(M)$, from the sample of M islands of the exact average size, $s_{av}(\infty)=s_{av}$. Then, one finds that

$$\begin{aligned} &E[s_{av}(M)] = s_{av}, \text{ and } V[s_{av}(M)] = A(s_{av})^2/M, \\ &A = \sigma^2 = \int_0^\infty (x-1)^2 f(x,t)dx. \end{aligned} \tag{C1}$$

Thus, for typical $\sigma^2=0.1$—0.2 and $M=100$, the standard error in $s_{av}(M)$ is only 3%–4% of s_{av}. Also of interest in this paper is the estimate, $\sigma^2(M)$, from a sample of M islands of the variance, $\sigma^2(\infty)=\sigma^2$, of the distribution f. One has that

$$\begin{aligned} &E[\sigma^2(M)] = \sigma^2(M-1)/M, \text{ and } V[\sigma^2(M)] = B/M, \\ &B = \int_0^\infty x^4 f(x,t)dx - \left[\int_0^\infty x^2 f(x,t)dx\right]^2. \end{aligned} \tag{C2}$$

for typical f where $\sigma^2=0.1$–0.2, one finds that $B=0.4$–1. Thus, for $M=100$, the standard error in $\sigma^2(M)$ is around 50% of σ^2!

[1] *Morphological Organization in Epitaxial Growth and Removal*, World Scientific Series in ''Directions in Condensed Matter Physics,'' Vol. 13, edited by Z. Zhang and M. G. Lagally (World Scientific, Singapore, 1998).
[2] J. A. Venables, Philos. Mag. **27**, 697 (1973); S. Stoyanov and K. Kashchiev, Curr. Top. Mater. Sci. **7**, 69 (1981); J. W. Evans and M. C. Bartelt, in Ref. 1.
[3] M. Zinke-Allmang, L. C. Feldman, and M. H. Grabow, Surf. Sci. Rep. **16**, 377 (1992).

[4] K. Morgenstern, G. Rosenfeld, and G. Comsa, Phys. Rev. Lett. **76**, 2113 (1996).
[5] G. Schulze Icking-Konert, M. Giesen, and H. Ibach, Surf. Sci. **398**, 37 (1998).
[6] J.-B. Hannon, C. Klunker, M. Giesen, H. Ibach, N. C. Bartelt, and J. C. Hamilton, Phys. Rev. Lett. **79**, 2506 (1998).
[7] J.-M. Wen, J. W. Evans, M. C. Bartelt, J. W. Burnett, and P. A. Thiel, Phys. Rev. Lett. **76**, 652 (1996); J.-M. Wen, S.-L. Chang, J. W. Burnett, J. W. Evans, and P. A. Thiel *ibid.* **73**, 2591 (1994).
[8] W. W. Pai, A. K. Swan, Z. Zhang, and J. F. Wendelken, Phys. Rev. Lett. **79**, 3210 (1997).
[9] M. von Smoluchowski, Phys. Z **17**, 585 (1916).
[10] K. Binder and M. H. Kalos, J. Stat. Phys. **22**, 363 (1980).
[11] A. F. Voter, Soc. Photo-Opt. Inst. Eng. **821**, 214 (1987).
[12] A. Bogicevic, S. Liu, J. Jacobsen, B. Lundqvist, and H. Metiu, Phys. Rev. B **57**, R9459 (1998); D. S. Sholl and R. T. Skodje, Phys. Rev. Lett. **75**, 3158 (1995); C. D. Van Siclen *ibid.* **75**, 1574 (1995); J. M. Soler, Phys. Rev. B **50**, 5578 (1994); H. C. Kang, P. A. Thiel, and J. W. Evans, J. Chem. Phys. **93**, 9018 (1990).
[13] J. Heinon, I. Koponen, J. Merikoski, and T. Ala-Nissila, Phys. Rev. Lett. **82**, 2733 (1999).
[14] S. V. Khare and T. L. Einstein, Phys. Rev. B **57**, 4782 (1998); **54**, 11752 (1996); S. V. Khare, N. C. Bartelt, and T. L. Einstein, Phys. Rev. Lett. **75**, 2148 (1995).
[15] R. Kern. G. Le Lay, and J. J. Metois, in *Current Topics in Materials Science*, edited by E. Kaldis (North Holland, Amsterdam, 1979), Chap. 3.
[16] W. B. Phillips, E. A. Deslodge, and J. G. Skofronick, J. Appl. Phys. **19**, 3210 (1968).
[17] E. Ruckenstein and B. Pulvermacher, J. Catal. **29**, 224 (1973).
[18] P. Meakin, Physica A **165**, 1 (1990).
[19] D. S. Sholl and R. T. Skodje, Physica A **231**, 631 (1996).
[20] H. Metiu, T. R. Mattsson, and G. Mills, in *Mechanisms and Principles of Epitaxial Growth in Metallic Systems*, edited by L. T. Wille, C. P. Burmester, K. Terakura, G. Comsa, and E. D. Williams (MRS, Pittsburgh, 1998), Vol. 528, p. 133; T. R. Mattsson, G. Mills, and H. Metiu, J. Chem. Phys. **110**, 12151 (1999).
[21] J. R. Sanchez and J. W. Evans, Phys. Rev. B **59**, 3224 (1999).
[22] Activation barriers for key PD processes (Refs. 11, 13, and 23) are roughly given by the sum of the barrier, E_e, for diffusion along $\langle 110 \rangle$ edges, and some multiple of an effective nearest-neighbor interaction. The terrace diffusion barrier satisfies $E_d \approx 2E_e$. The vacancy diffusion barrier, E_v, is set equal to E_e in Ref. 13, but it is likely higher. For Cu/Cu(100), one has $E_v=0.44$, $E_e=0.25$, $E_d=0.43$ [EMT (Ref. 24)]; $E_v=0.42$, $E_d=0.52$ [GGA (Ref. 25)]. For Ag/Ag(100), one has $E_v=0.42$, $E_e=0.25$, $E_d=0.37$ [EMT (Ref. 24)]; $E_v=0.46$, $E_e=0.26$, $E_d=0.49$ [EAM (Ref. 11)]. All energies are in eV.
[23] C. R. Stoldt, A. M. Cadilhe, C. J. Jenks, J.-M. Wen, J. W. Evans, and P. A. Thiel, Phys. Rev. Lett. **81**, 2950 (1999).
[24] P. Stoltze, J. Phys.: Condens. Matter **6**, 9495 (1994).
[25] G. Boisvert and L. J. Lewis, Phys. Rev. B **56**, 7643 (1997).
[26] D. Kandel, Phys. Rev. Lett. **79**, 4238 (1997).
[27] M. C. Bartelt and J. W. Evans, Surf. Sci. **298**, 421 (1993); Phys. Rev. B **46**, 12675 (1992).
[28] M. C. Bartelt and J. W. Evans, Phys. Rev. B **54**, R17359 (1996).
[29] M. C. Bartelt, C. R. Stoldt, C. J. Jenks, P. A. Thiel, and J. W. Evans, Phys. Rev. B **59**, 3125 (1999).
[30] L. Bardotti, M. C. Bartelt, C. J. Jenks, C. R. Stoldt, J.-M. Wen, C.-M. Zhang, P. A. Thiel, and J. W. Evans, Langmuir **14**, 1487 (1998).
[31] C.-M. Zhang, M. C. Bartelt, J.-M. Wen, C. J. Jenks, J. W. Evans, and P. A. Thiel, Surf. Sci. **406**, 178 (1998).
[32] D. W. McComb, B. A. Collings, R. A. Wolkow, D. J. Moffatt, C. D. MacPherson, D. M. Rayner, P. A. Hackett, and J. E. Hulse, Chem. Phys. Lett. **251**, 8 (1996); T. Michely and G. Comsa, in Ref. 1.
[33] G. Oshanin, M. Moreau, and S. Burlatsky, Adv. Colloid Interface Sci. **49**, 1 (1994).
[34] C. R. Stoldt, A. M. Cadilhe, M. C. Bartelt, C. J. Jenks, P. A. Thiel, and J. W. Evans, Prog. Surf. Sci. **59**, 67 (1998).
[35] In Ref. 7, the estimate of τ was based the number of hops required for an atom (random walker) to visit of the order of $(L_{\text{edge}})^2$ sites. However, not all these sites need be visited for a cluster to collide with another cluster, since clusters are extended objects.
[36] M. C. Bartelt, S. Gunther, E. Kopatzki, R. J. Behm, and J. W. Evans, Phys. Rev. B **53**, 4099 (1996).
[37] C. Ratsch, A. Zangwill, P. Smilauer, and D. D. Vvedensky, Surf. Sci. **329**, L599 (1995).
[38] E. Bauer, Z. Kristallogr. **110**, 372 (1958).
[39] H. Roeder, K. Bromann, H. Brune, and K. Kern, Surf. Sci. **376**, 13 (1997).
[40] C. Ratsch, A. Zangwill, and P. Smilauer, Surf. Sci. **314**, L937 (1994). For near-square islands, the strain energy is reasonably estimated from a 1D Frenkel-Kontorova theory treating the island as a composite of noninteracting 1D adatom chains.
[41] M. Schroeder and D. E. Wolf, Surf. Sci. **375**, 129 (1997).
[42] C. Ratsch, P. Ruggerone, and M. Scheffler, in Ref. 1.
[43] J. de la Figuera, J. E. Prieto, C. Ocal, and R. Miranda, Solid State Commun. **89**, 815 (1994).
[44] J. C. Hamilton, Phys. Rev. Lett. **77**, 885 (1996).